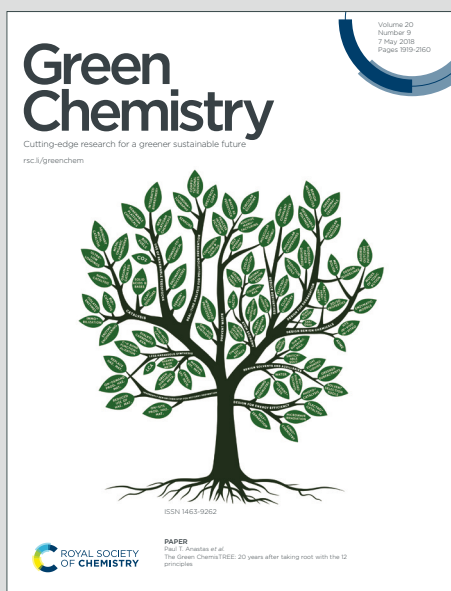


Green Chemistry

Cutting-edge research for a greener sustainable future

Accepted Manuscript

This article can be cited before page numbers have been issued, to do this please use: C. Cova, A. Zuliani, M. J. Muñoz-Batista and R. Luque, *Green Chem.*, 2019, DOI: 10.1039/C9GC01596E.



This is an Accepted Manuscript, which has been through the Royal Society of Chemistry peer review process and has been accepted for publication.

Accepted Manuscripts are published online shortly after acceptance, before technical editing, formatting and proof reading. Using this free service, authors can make their results available to the community, in citable form, before we publish the edited article. We will replace this Accepted Manuscript with the edited and formatted Advance Article as soon as it is available.

You can find more information about Accepted Manuscripts in the [Information for Authors](#).

Please note that technical editing may introduce minor changes to the text and/or graphics, which may alter content. The journal's standard [Terms & Conditions](#) and the [Ethical guidelines](#) still apply. In no event shall the Royal Society of Chemistry be held responsible for any errors or omissions in this Accepted Manuscript or any consequences arising from the use of any information it contains.

Efficient scrap waste automotive converter Ru-based catalysts for the continuous-flow selective hydrogenation of cinnamaldehyde

Camilla Maria Cova,^a Alessio Zuliani,^a Mario J. Muñoz-Batista^{a*} and Rafael Luque^{a,b*}

Received 00th January 20xx,
Accepted 00th January 20xx

DOI: 10.1039/x0xx00000x

www.rsc.org/

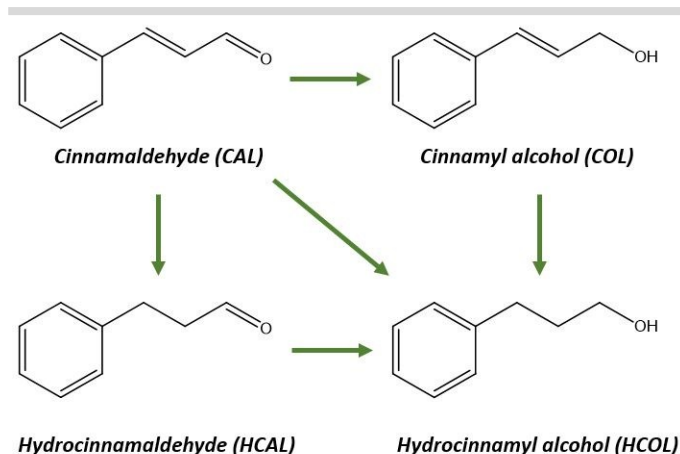
The selective, efficient and sustainable continuous flow hydrogenation of a α,β -unsaturated aldehyde, *i.e.* cinnamaldehyde, to the corresponding unsaturated alcohol, *i.e.* cinnamyl alcohol, using a scrap waste automotive converter novel Ru-based catalyst is reported. The catalyst was prepared by recycling and upgrading waste ceramic-cores of scrap automotive catalytic converters as supporting material. Ruthenium was incorporated in the ceramic structures using a simple, fast and solventless mechanochemical-assisted procedure followed by a chemical reduction step. Different catalysts were prepared varying Ru content. The materials were characterized by XRD, N₂ physisorption, XPS, TEM, HRTEM and SEM/mapping analyses. Compared to Ru supported over most studied silica and alumina supports, the new system displayed outstanding catalytic performance under continuous-flow conditions in terms of conversion and selectivity as well as a remarkable stability with time-on-stream, demonstrating a synergistic action between Ru and the waste catalytic converter support. A Ru loading of 10 wt.% provided optimum results, including a cinnamaldehyde conversion up to 95% with a selectivity to cinnamyl alcohol of 80%.

1. Introduction

Chemo-selectivity is a bedrock of catalytic processes since it involves the activation of specific functional groups within more complex starting reactants. The chemo-selective hydrogenation of α,β -unsaturated aldehydes represents a critical step in the synthetic preparation of chemicals for the pharmaceutical and flavour/fragrance industry. For example, citral, an α,β -unsaturated aldehyde extracted from plants, can be selectively hydrogenated to geraniol, a commonly used fragrance tasting of peach, raspberry, grapefruit and red apple.¹⁻⁵ In general, the chemo-selective hydrogenation of α,β -unsaturated aldehydes has been widely investigated from a mechanistic point using different catalytic systems.⁶⁻⁸ The results demonstrated that the activation of the double carbon bond is kinetically and thermodynamically favoured, leading to the formation of saturated aldehydes.^{1, 9-11} However, the less-favoured unsaturated alcohols ($\Delta E \sim 35 \text{ kJ mol}^{-1}$ less favoured)¹² are of high value and broadly employed in industry.^{10, 13-15} As a consequence, the design of catalytically active materials that preferentially hydrogenates the carbonyl bond with in yields is a captivating yet significant challenge still nowadays.

A largely investigated reaction for the selective hydrogenation of α,β -unsaturated aldehydes is the hydrogenation of

cinnamaldehyde (CAL) to cinnamyl alcohol (COL). COL is a fragrance smelling as hyacinth with balsamic and spicy notes widely used in perfumes, drugs and in food formulations.¹⁶⁻¹⁸ As illustrated in Scheme 1, besides COL, the other principal products of the hydrogenation of cinnamaldehyde include hydrocinnamaldehyde (HCAL) and hydrocinnamyl alcohol (HCOL).¹⁹⁻²¹



Scheme 1 Reaction pathways in the hydrogenation of cinnamaldehyde (CAL: cinnamaldehyde; COL: cinnamyl alcohol; HCAL: hydrocinnamaldehyde; HCOL: hydrocinnamyl alcohol)

Most studied chemo-selective heterogeneous catalysts for the hydrogenation of CAL to COL are based on supported ruthenium compounds.²²⁻²⁵ In particular, significant conversion and selectivity values have been reported using

^a Departamento de Química Orgánica, Universidad de Córdoba, Edificio Marie-Curie (C-3), Ctra Nnal IV-A, Km 396, Córdoba, Spain. E-mail: rafael.luque@uco.es

^b Peoples Friendship University of Russia (RUDN University), 6 Miklukho Maklaya str., 117198, Moscow, Russia

ruthenium supported on porous alumina²⁶ or silica.²⁷ More recently, also different carbon materials such as graphene,²⁸ carbon nanotubes,^{22, 29, 30} activated carbons^{31, 32} or mesoporous carbons³³ have been reported as efficient supporting materials. The choice of an appropriate supporting material is of primary importance since its intrinsic properties and, more importantly, the interaction between the metals and the support can deeply modify the reaction selectivity, as reported by Leng et al.³⁴ Firstly, a lower metal dispersion generally boosts the selectivity to COL. Furthermore, an enhanced charge transfer between the metal and the support material can also lead to an improvement of selectivity to COL. Finally, the presence of metallic promoters or additional Lewis acid properties could also endorse the selectivity to COL.

Important features that should always be considered in the development of novel supporting materials include the scalability and the green credentials of the reaction. Therefore, new supporting materials should be inexpensive, easily synthesized and have low environmental impact.

Within these aims, the exploitation of largely-produced waste can offer almost unlimited opportunities. In 2016, ca. 6 million of end-of-life vehicles were registered only in the European Union, generating approximately 6 thousand tons of ceramic-cores of scrap automotive catalytic converters (CATs). Scrap CATs are normally recycled and treated in order to recover platinum-group metals (PGMs). However, these procedures are normally highly toxic, time consuming and generates lots of waste.³⁵⁻⁴⁰ In addition, also the latest procedures with environmental friendly characteristics still have very high E-factor, as only the PMGs are recovered, while the remaining matrix is waste.⁴¹

Herein, novel Ru catalysts supported on scrap waste CATs with high catalytic activity (up to 95% conversion) and selectivity (up to 80%) in the hydrogenation of CAL to COL are reported. To the best of our knowledge, no similar works were previously described on the use of these systems as sustainable catalyst supports. Ru-based catalysts were prepared via fast and simple procedure involving a mechanochemical step followed by a chemical reduction. The catalysts were tested in the hydrogenation of CAL to COL using a continuous flow system to test not only activity and selectivity of the systems but also their stability with time-on-stream. Remarkably, IUPAC has identified flow chemistry and mechanochemistry among the “top ten chemical innovations that will change our world” and defined them as “emerging technologies with potential to make our planet sustainable”.⁴² Indeed, continuous flow systems can offer several advantages including the use of small amounts of solvents and chemical reagents, reduced reaction times, improved selectivity and increased yields.^{43, 44} On the other hand, mechanochemical protocols allow to carry out reactions easily, quickly, with high reproducibility, avoiding, in most cases, solvent utilization. As a result, mechanochemistry can be pointed as an overall highly relevant environmentally-friendly technique.⁴⁵⁻⁴⁷

2. Experimental sections

Ruthenium(III)-chloride hydrate ($\text{RuCl}_3 \cdot x\text{H}_2\text{O}$), sodium borohydride (NaBH_4 , 99%), trans-cinnamaldehyde ($\text{C}_9\text{H}_8\text{O}$, 99%) and ethanol ($\text{CH}_3\text{CH}_2\text{OH}$, 99.5%) were purchased from Sigma-Aldrich Inc., St. Louis, MO, USA. Acetonitrile (CH_3CN , 99.9%), silica Gel 60 (63-200 microns), aluminium oxide basic, aluminium oxide activated acidic were purchased from PanReac Química, Barcelona, Spain. All reagents were used without any further purification.

2.1 Synthesis

Prior to the utilization as supporting material, the ceramic-cores of scrap automotive catalytic converters (CATs), kindly donated by the company PROVALUTA S.L., were washed and dried. Specifically, 50 g of CATs were dispersed in 100 mL of distilled water and put in an ultrasonic bath for 2 hours. Sequentially, the powders were filtrated and dried in a 100°C oven (the resulting powder was denoted as CCO, unreduced support).

A number of supported Ru catalysts were synthesized (supporting materials: CCO, SiO_2 , Al_2O_3 activated or Al_2O_3) by a mechanochemical-assisted method followed by a chemical reduction. In a typical synthesis, the supporting powder (2 g) and the correct amount of ruthenium salt, $\text{RuCl}_3 \cdot x\text{H}_2\text{O}$, (456 mg for 10%wt; 228 mg for 5%wt, 114 mg for 2.5%wt and 45 mg for 1%wt) were mixed together in a 125 mL stainless steel milling jar equipped with eighteen 5 mm diameter stainless steel balls. The powders were grounded in a Retsch PM100 planetary ball mill at 350 rpm for 15 minutes, changing the direction of rotation every 2'30". Upon milling, the resulting homogenous powders were chemically reduced using NaBH_4 (4 eq) and EtOH (20 mL) as solvent. The reduced catalysts were filtrated and washed with water (5 mL) and ethanol (5 mL). Finally, the resulting powders were oven-dried at 100°C for 24 hours. Samples were named 10%Ru/CC, 5%Ru/CC, 2.5%Ru/CC, 1%Ru/CC, 0%Ru/CC (0%Ru/CC has no ruthenium content, standing for reduced CCO), 10%Ru/ SiO_2 , 10%Ru/ Al_2O_3 activated and 10%Ru/ Al_2O_3 . CCO corresponds to the unreduced/untreated scrap CAT.

2.2 Catalyst characterization

Powder X-ray diffraction (XRD) patterns were obtained with a Bruker D8 DISCOVER A25 diffractometer (PanAnalytic/Philips, Lelyweg, Almelo, The Netherlands) using $\text{CuK}\alpha$ ($\lambda = 1.5418\text{\AA}$) radiation. Wide angle scanning patterns were collected over a 2θ range from 10° to 80° with a step size of 0.018° and counting time of 5 s per step.

Textural properties of the samples were determined by N_2 physisorption using a Micromeritics ASAP 2020 automated system (Micromeritics Instrument Corporation, Norcross, GA, USA) using the Brunauer-Emmet-Teller (BET) and the Barret-Joyner-Halenda (BJH) methods. The samples were outgassed for 24 h at 100 °C under vacuum ($P_0 = 10^{-2}$ Pa) and subsequently analysed.

Scanning electron microscopy images were recorded with a JEOL JSM-6300 scanning microscope (JEOL Ltd., Peabody, MA, USA) equipped with Energy-dispersive X-ray spectroscopy

(EDX) at 15 kV at the Research Support Service Center (SCAI) from University of Cordoba.

TEM images were recorded in a JEOL 1200 equipped with Energy-dispersive X-ray spectroscopy (EDX), at the Research Support Service Center (SCAI) from Universidad de Cordoba. Prior to analysis, samples were prepared by suspension in EtOH, assisted by sonication and followed by deposition on a copper grid.

HRTEM images were recorded in a FEI TITAN³ (CEOS Company) equipped with a SuperTwin[®] objective lens and a CETCOR Cs-objective corrector (CEOS Company) at the Laboratorio de Microscopias Avanzadas of the Instituto de Aragon, at the University of Zaragoza (Spain).

XPS studies were performed at the Central Service of Research Support (SCAI) of the University of Cordoba, using an ultrahigh vacuum (UHV) multipurpose surface analysis system Specs[™]. The experiments were carried out at pressures $<10^{-10}$ mbar, using a conventional X-ray source (XR-50, Specs, Mg-K α , $h\nu = 1253.6$ eV, $1 \text{ eV} = 1.603 \times 10^{-19}$ J) in a "stop and go" mode. The samples (4 mm x 4 mm pellets, 0.5 mm thick) were evacuated overnight under vacuum ($<10^{-6}$ mbar). Spectra were collected at room temperature (pass energy: 25 and 10 eV, step size: 1 and 0.1 eV) with a Phoibos 150-MCD energy detector. The deconvolutions of the curves and the elements quantifications were obtained using XPS CASA software.

2.3 Catalytic experiments

Catalytic performances of the catalysts were evaluated under liquid phase continuous flow conditions in an H-Cube Mini Plus[™] flow hydrogenation reactor. The materials were packed (~ 0.2 g of catalyst per cartridge) in 30 mm-long ThalesNano CatCarts. Initially, the reactor was washed with methanol and acetonitrile (0.3 mL min⁻¹ flow, 20 minutes for each solvent). Sequentially, a solution of 0.1 M cinnamaldehyde in acetonitrile was pumped through and the reaction conditions were optimized basing on previous studies from the group (90°C, 30 bar, 0.1 mL min⁻¹). The required hydrogen was generated *in situ* during the reaction by water electrolysis in the H-Cube equipment. The reactions were performed for 120 minutes, collecting samples every 15 minutes for further analysis. Samples collected at "0 min" were considered as first outcomes under operative reaction conditions passed through the cartridge.

The conversion and selectivity were analyzed by gas chromatography (GC) in an Agilent 6890N gas chromatograph (60 mL min⁻¹ N₂ carrier flow, 20 psi column top head pressure) using a flame ionization detector (FID). A capillary column Agilent Technologies Inc. HP-5 (30 m x 0.32 mm x 0.25 μ m) was employed. Calibration curve was obtained with an internal standard method using octane as standard. Standard solutions of cinnamaldehyde (from 0.005 to 0.1 M) and 0.1 M octane in CH₃CN were analyzed by GC to give linear regressions with $R^2 > 0.999$. In addition, the collected liquid fractions were analyzed by GC-MS—using the Agilent 7820A GC/5977B High Efficiency Source (HES) MSD—in order to identify the obtained products.

3. Results and discussion

View Article Online

DOI: 10.1039/C9GC01596E

3.1 Characterization of Ru/catalytic converter systems

The novel catalysts were characterized by XRD, TEM, HRTEM, SEM/mapping, N₂ physisorption and XPS. As illustrated in Fig.1, the washing of the starting CATs for the preparation of CC resulted in incrementing the diffraction peaks of the samples. This demonstrated that a great portion of the amorphous carbon adsorbed on the surfaced was successfully removed. Considering samples CC0 (unreduced support), 0%Ru/CC (reduced CC0) and 10%Ru/CC, the most intense diffraction peaks observed at 2θ values of 21.72°, 28.49° and 54.67° could be indexed to the (1 0 0), (0 1 1), (2 0 2) planes of SiO₂ with hexagonal structure (JCPDS 00-023-0961), one of the major component of CATs.⁴⁸

In fact, an automotive catalytic converter generally consists of four main structures:⁴⁹

- 1) The catalyst core or substrate, which consists of a ceramic monolith (defined as inner ceramic). The monolith has a honeycomb structure mainly made of cordierite (2MgO·2Al₂O₃·5SiO₂).
- 2) The wash coat, which is a carrier for the catalytic material and is used to disperse the materials over a large surface area. Al₂O₃, TiO₂, SiO₂, or a mixture of alumina and silica can be used.
- 3) CeO₂ or CeO₂-ZrO₂. These oxides are mainly added to promote the oxygen storage adsorbed from air and needed for the oxidations of exhaust emission.
- 4) Noble metals such as platinum, palladium and rhodium. Other metals such as iron, manganese, nickel and cerium are also present.

As a consequence of this complexity, all remaining diffraction peaks could hardly be assigned in any case due to their low diffraction line intensities. ICP-MS of CC0 unreduced support also detected Si, Al, Mg, Fe and Ce as main components while also minor components such as Ti, Zn, Zr and Pt were revealed. (For detailed ICP-MS analysis please see ESI, Table S.1).

XRD patterns of 10%Ru/CC, as well as the XRD pattern of 10%Ru/SiO₂, 10%Ru/Al₂O₃ and 10%Ru/Al₂O₃ activated did not show any appreciable peaks that could be indexed to ruthenium. (Please see ESI Fig.S.1 for the complete XRD patterns) The presence of Ru was subsequently confirmed by TEM, HRTEM, SEM/mapping and XPS analysis.

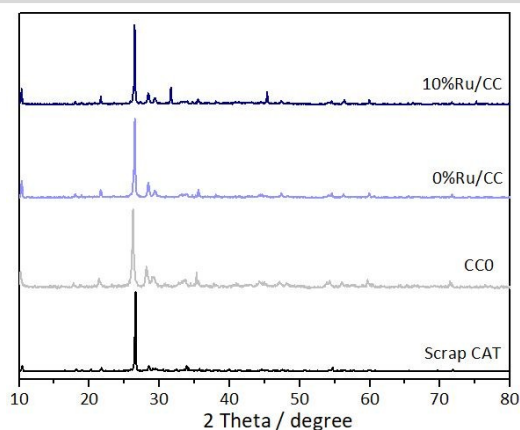


Fig. 1 XRD patterns for 10%Ru/CC, 0%Ru/CC, CCO and ceramic-core of scrap catalytic converter

Fig.2 shows SEM images and SEM/mapping of sample 10%Ru/CC. In Fig.2-A it is possible to visualise flakes structures derived from the smashed ceramic honeycomb. Fig.2-B,C and D show the EDX-mapping of the major components of the CC support, *i.e.* C, Si and Al. The inhomogeneous carbon distribution is a consequence of the ball milling treatment: initially, carbon was almost exclusively located on the CATs surface, while mixed with all other components after ball milling. Si and Al were homogeneously distributed over the catalyst surface, as they are elements both present in the catalyst core and in the wash coat. Remarkably, as illustrated in Fig.2-E, Ru was homogeneously-distributed over all the catalyst surface. (Fig. S.2 ESI, SEM/mapping of all samples).

Fig.3 shows TEM images of scrap automotive catalytic converter (CATs) and of 10%Ru/CC catalyst before and after the catalytic tests. TEM images of 10%Ru/CC catalyst (Figures 3-B,C) showed that ruthenium particles were successfully supported on the catalytic converter surface. In particular, several darker areas, clearly associated with the ruthenium-oxide counterpart, were observed and confirmed by EDX analysis. Despite some significant agglomeration takes place (Fig.3-C), the materials were proved to be highly active and stable under the investigated reaction conditions.

In order to better analyse the morphology and Ru content of 10%Ru/CC, additional HRTEM images were taken as illustrated in Fig.4. The images showed the smashed structure of CATs (Fig.4-A, Fig.4-B) and the presence of Ru nanoparticles, also in some agglomerated forms (Fig.4-C and Fig.4-D). The dimension of individual Ru nanoparticles were found to be ca. 2 nm diameter (Fig.4-E). The d-spacing of some of the ruthenium crystals ranged from 0.20 to 0.21, which can be associated to the (101) and (002) planes of RuO₂ (for additional images, please see ESI, Fig.S.3).

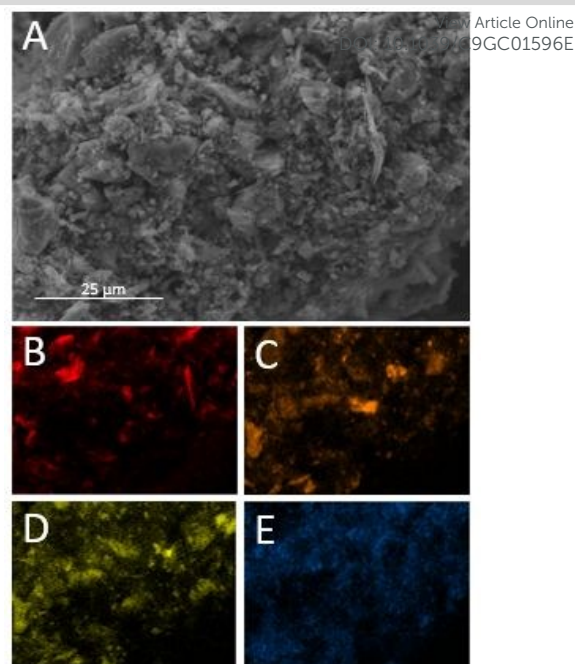


Fig. 2 (A) SEM image of the 10%Ru/CC catalyst with mapping analysis of (B) Carbon; (C) Silicon; (D) Aluminium and (E) Ruthenium

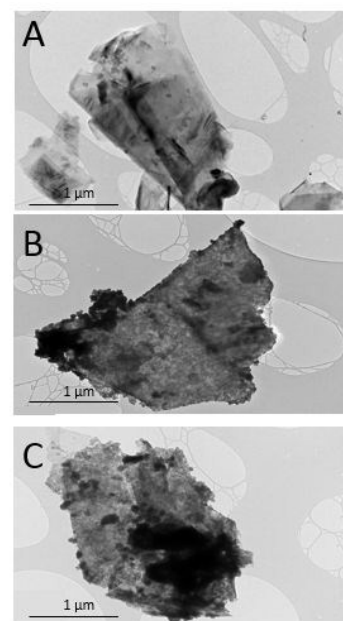


Fig. 3 TEM images of the CATs (A), 10%Ru/CC catalyst (B) and 10%Ru/CC catalysts after stability test (C)

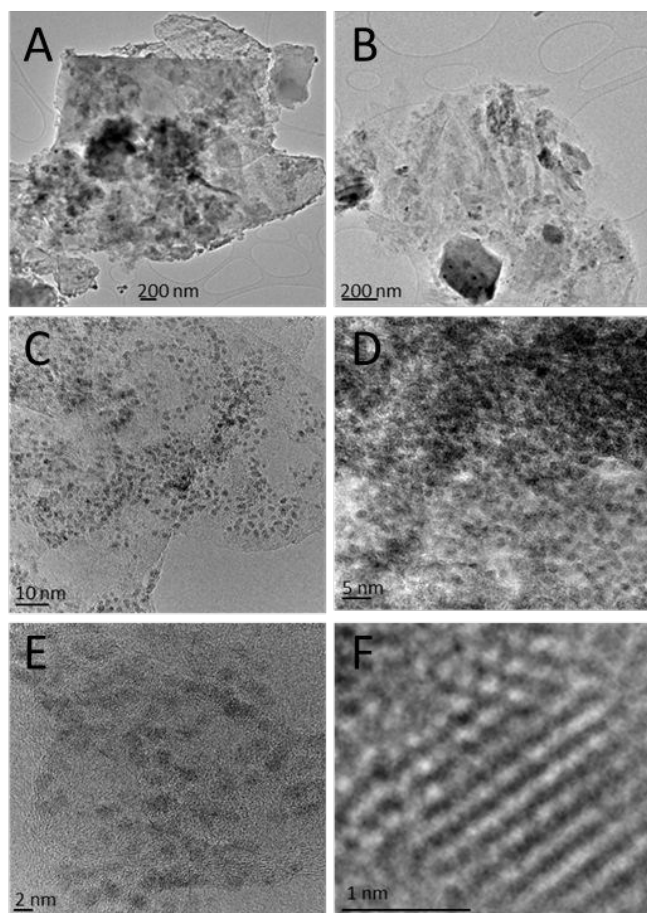


Fig. 4 HRTEM images of 10%Ru/CC. F corresponds to a single Ru nanoparticle

In order to determine the specific surface area of the catalyst, Brunauer–Emmett–Teller (BET) physisorption was carried out by nitrogen adsorption–desorption measurements. Table 1 lists the results of the analysis. The data demonstrated that the catalysts were essentially non porous (Type III Isotherm), in good agreement with SEM images. After the addition of ruthenium, a slight increasing in surface area was observed. This could be related to the ball-milling addition of the ruthenium precursor which was deposited on the surface of the catalytic converter as small nanoparticles, increasing the surface area. After metal reduction, these particles were reduced in dimensions so that a further surface area increment was detected (Please see the isotherm graph in the ESI, Fig.S.4).

Table 1 Textural properties of key synthesized catalysts

Sample	Surface area / $\text{m}^2 \text{g}^{-1}$
CCO (unreduced support)	13
10%Ru/CC*	16
10%Ru/CC	21

*before chemical reduction

The interaction of Ru entities and the CC support was also studied by XPS. As analysed in previous work, Ru-containing

catalysts exhibit complex spectra. On the one hand, the fitting of the Ru 3d core level can be achieved using several asymmetric lines shape, on the other hand, a strong overlapping effect from close enough peak positions can be encountered between carbon and ruthenium contributions.^{50, 51} Such overlapping can be observed in Fig.5-A. Ru 3d XPS region showed a separate band at 280.7 eV, which can be associated with a dominant Ru (IV) oxidation state on the surface.⁵⁰ Position and shape of this contribution were pretty like the obtained for the 10%Ru/SiO₂ reference (Fig.5-A). However, clear differences concerning the C component were observed. C 1s, with a reference peak at 284.6 eV (C–C), confirmed that adventitious C remained in the structure of the CC support after the washing treatments and the further functionalization with Ru.

A detailed analysis of the region is presented in Fig.5-C for the 10%Ru/CC sample. The fitting procedure followed recommendations given by Morgan.⁵⁰

Fig.5-C shows the lines at 284.7 eV ($3d_{5/2}$) and 284.0 eV ($3d_{3/2}$) associated, as aforementioned, with RuO₂.^{50, 51} In addition, satellites 1.9 eV above each Ru (3d) signal and line shape equivalent to the parent peak and a spin-orbit splitting of 4.17 eV for photoelectron peaks and satellites with an area ratio of 0.67 must be considered.⁵⁰ The existence of dominant oxidized ruthenium was confirmed by Ru 3p XPS region.

As observed in Fig.5-B and Fig.5-D, the binding energy values associated with the Ru $3d_{3/2}$ peak were both (10%Ru/CC and 10%Ru/SiO₂) above 462.7 eV, characteristic of Ru(IV).^{52, 53} Identification of other elements constituting the CC structure and silica support was also carried out. Fig.5-E,F and G show the Si 2p, O 1s and Al 2s XPS regions. The values of ca. 103.6 eV and 533.1 eV agree with Si 2p and O 1s of SiO₂, respectively.⁵⁴ Nonetheless, all Si 2p, O 1s as well as Al 2s showed a low binding energy shift in comparison with pure aluminosilicate compounds,⁵⁵ which could be associated with an electronic effect due to the presence of multiple Si- and O-metals (Ce, Zr, Fe, etc.) interactions in the CC support.

However, no clear evidence of charge transfer enhancement and its relation with the activity and selectivity could be claimed from this result,³⁴ and new experiments such as in-situ synchrotron X-ray absorption spectroscopy must be considered to evidence this singular interaction.

Finally, 10%Ru/CC catalyst was characterized by XPS analysis after the stability test, showing no appreciable differences compared with the fresh (unused) catalyst.

3.2 Catalytic tests

Influence of flow rate

The effect of the flow rate on the hydrogenation of CAL was initially investigated using 5%Ru/CC and 10%Ru/CC. Previously optimised operating conditions of 90°C temperature under 30 bar H₂ pressure were selected as starting conditions.⁵⁶ Acetonitrile was chosen as solvent due to the less aggressive toxic and pollutant characteristics⁵⁷ as well as being optimum solvent for the hydrogenation of CAL in previous work from the group.⁵⁸ Other solvents including isopropanol, ethanol and water were discharged due to relevant problems in flow

conditions such as cartridge blockage and pressure drop issues. Fig.6 displays the results in terms of conversion and selectivity to COL operating at flow rates of 0.1, 0.3 and 0.6 mL min⁻¹. Steady state conditions were observed for all catalysts after 45' of reactions.

Table 2 summarizes the results in average under steady-state conditions. Main products include COL, CAL and HCAL. Other products (reported together as "others") include β -methylstyrene, propylbenzene and ring hydrogenation products.⁵⁸ While a higher content of Ru provided a higher conversion (Fig.6-A and Table 2), the correlation between Ru% and selectivity to COL was not obvious. Reduced Ru content corresponded to an increased selectivity to COL of ca. 5-10% at

a flow rate of 0.1 mL min⁻¹ and 0.3 mL min⁻¹. As HCAL was not observed (Table 2), although there is no experimental evidence, the most probable hypothesis is that CAL was initially hydrogenated to COL, which was subsequently hydrogenated to HCOL. This supposition could be further supported by the observed selectivity to COL at higher flow rates (e.g. 0.6 mL min⁻¹). Higher flux prevented a longer contact between COL and the catalyst, avoiding the sequential hydrogenation to HCOL. In order to better analyse the selective hydrogenation to COL, the flow rate of 0.1 mL min⁻¹ was further selected (Table 2).

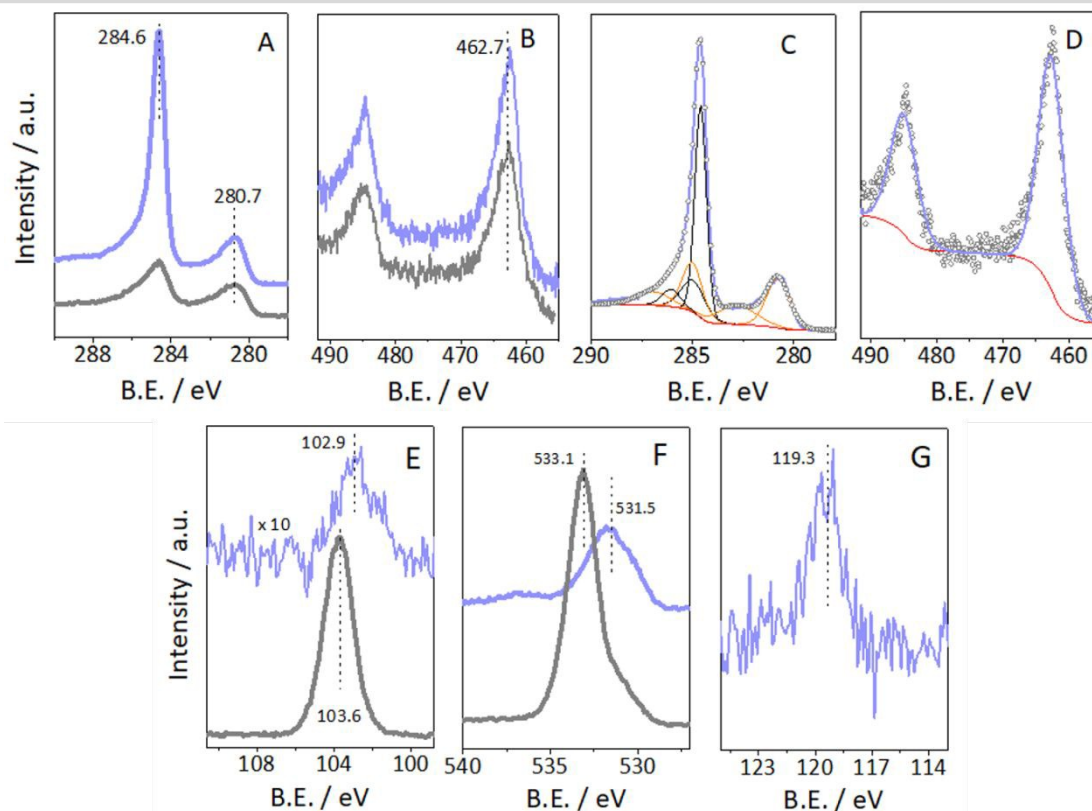


Fig. 5 XPS analysis of 10%Ru/CC (light blue) and 10%Ru/SiO₂ (grey) samples. (A) C 1s and Ru 3d. (B) Ru 3p. (C) Representative example (10%Ru/CC) of the fitting procedure of C 1s (black) and Ru 3d (orange) XPS regions. (D) Representative example (10%Ru/CC) of the fitting procedure of Ru 3p XPS region. (E) Si 2p. (F) O 1s and Al. (G) Al 2s

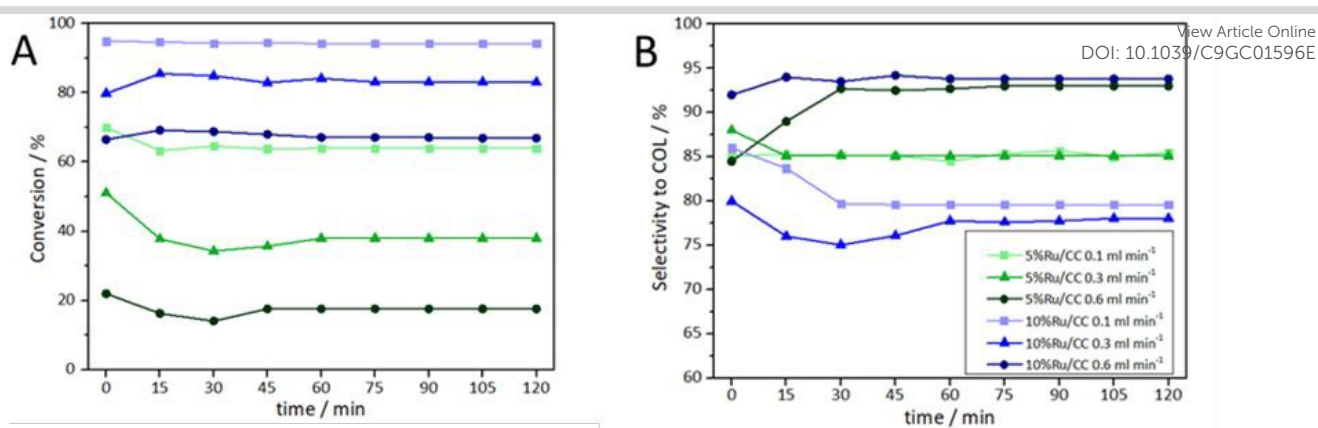


Fig. 6 Influence of the flow rate on CAL conversion (A) and COL selectivity (B). Reaction conditions: $p = 30$ bar H_2 ; $T = 90^\circ C$

Table 2 Reaction parameters and conversion and selectivity values at steady state conditions for the reaction carried out at different flow rates

Catalyst	Flow rate / $ml\ min^{-1}$	τ / min*	Conversion / %	Selectivity / %				COL Yield / %
				COL	HCAL	HCOL	Others	
BLANK	0.1	3	<3%	-	-	-	-	-
10%Ru/CC	0.1	3	94.4	80.1	-	8.8	11.1	75.6
10%Ru/CC	0.3	1.5	84.8	74.2	-	6.1	19.7	62.9
10%Ru/CC	0.6	0.7	64.8	93.4	-	-	6.6	60.5
5%Ru/CC	0.1	3	64.0	85.1	-	5.1	9.8	54.5
5%Ru/CC	0.3	1.5	38.0	85.0	-	3.8	11.2	32.3
5%Ru/CC	0.6	0.7	19.9	92.2	-	-	7.8	18.3

*residence time = Catcarts volume / flow rate

Table 3 Reaction parameters and conversion and selectivity values at steady state conditions for the reaction carried out at different H_2 pressures

Catalyst	Pressure / bar	Temperature / $^\circ C$	Conversion / %	Selectivity / %				COL Yield / %
				COL	HCAL	HCOL	Others	
10%Ru/CC	10	90	38.2	84.1	-	6.7	9.2	32.1
10%Ru/CC	20	90	66.4	82.7	-	7.0	10.3	54.9
10%Ru/CC	30	90	94.4	80.1	-	8.8	11.1	75.6
10%Ru/CC	40	90	95.1	79.9	-	9.2	10.9	75.9

Table 4 Reaction parameters and conversion and selectivity values at steady state conditions for the reaction carried out at different temperatures

Catalyst	Pressure / bar	Temperature / $^\circ C$	Conversion / %	Selectivity / %				COL Yield / %
				COL	HCAL	HCOL	Others	
10%Ru/CC	30	50	78.3	68.9	-	16.6	14.5	53.9
10%Ru/CC	30	70	85.6	74.2	-	11.4	12.4	63.5
10%Ru/CC	30	90	94.4	80.1	-	8.8	11.1	75.6

Influence of H_2 pressure and temperature

The influence of the H_2 pressure and temperature on the hydrogenation of CAL was further studied using 10%Ru/CC. A set of experiments were carried out fixing the reaction temperature at $90^\circ C$ and varying the H_2 pressure (from 10 to

40 bar). Steady state conditions were observed for all trials after 45 mins of reaction (ca. 2 mins residence time).

Table 3 summarizes average results under steady-state conditions. Remarkably, the selectivities to the main different products gave almost the same values. However, a higher

pressure provided a higher conversion, reaching a maximum at 30 bar of H₂ pressure. The experiment conducted at 40 bar of H₂ pressure gave almost identical results. As a result, 30 bar H₂ pressure value was selected as optimum reaction pressure, in order to minimize the energy consumption. Successively, a sequence of experiments was carried out operating at 30 bar H₂ pressure and changing the reaction temperature. The trials were performed at 50, 70 and 90 °C. 90 °C was selected as maximum reaction temperature in order to operate avoiding any damage and blockage of the instrument (H-Cube can operate maximum at 100 °C). Results at steady-state conditions are presented in Table 4.

A higher temperature provided higher conversion and higher selectivity to COL. Based on these results (94% of conversion and 80% of selectivity to COL), 90 °C was selected as optimum reaction temperature.

Effect of Ruthenium loading

Sequentially, operating under optimized flow rate of 0.1 mL min⁻¹, the selective hydrogenation of CAL was investigated as function of the metal loading. As illustrated in Fig.7, optimum conversion values were observed at higher Ru contents, with very low conversion obtained for Ru loadings below 5% Ru.

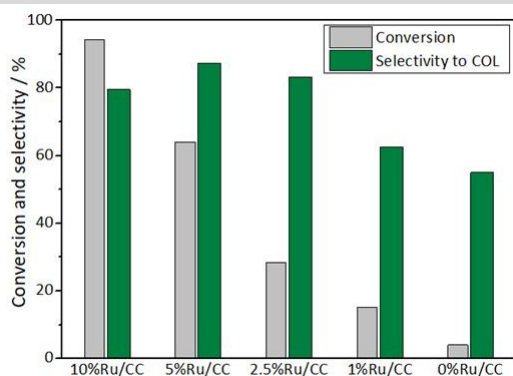


Fig. 7 CAL conversion and COL selectivity average under steady state conditions (TOS = 120 min) for different Ruthenium loadings over CC supporting material. Reaction conditions: p = 30 bar H₂; T = 90 °C; flow rate = 0.1 mL min⁻¹

In addition, the selectivity to COL increased by increasing Ru content, reaching a maximum for 5%Ru/CC. As previously described, sample 10%Ru/CC showed slightly less selectivity to COL due to further hydrogenation to HCOL (Table 2). Despite catalyst 5%Ru/CC showed the best performance in terms of selectivity, 10%Ru/CC was selected for sequential tests due to the optimum product yield (75% vs 54% for 5%Ru/CC, Table 2). Remarkably, CC (reduced) support material showed some catalytic activity also before addition of Ru, while CC0 (support

not reduced) showed no catalytic activity. This can be explained in terms of the content of noble metals in the supporting material: after the recovery and the washing of the ceramic from scrap automotive catalytic converters, noble metals (Pt, Pd, Rh) present in trace quantities in CATs were also reduced during the reduction of Ru, reactivating the metallic sites. As described by Gallezot and Richard⁹, Pt is highly selective to the carbonyl group, while Pd to the olefinic bond, explaining the selectivity to COL of 1%Ru/CC and reduced CC samples of around 62% and 50%, respectively (ESI, see Table S.2 for all selectivity and yield data).

Influence of the supporting material

In order to investigate and demonstrate the positive influence of the CC supporting material on the catalytic activity, different catalysts (10%Ru loading) were prepared using standard supporting materials including SiO₂, acidic Al₂O₃ activated and commercial Al₂O₃. As illustrated in Fig.8 and Table 5, the conversion obtained for 10%Ru/CC was remarkably superior to that of all additionally investigated supports.

The most active alternative catalyst, 10%Ru/SiO₂, exhibited a conversion of CAL up to 68.4% but with low selectivity to COL (32.4%).

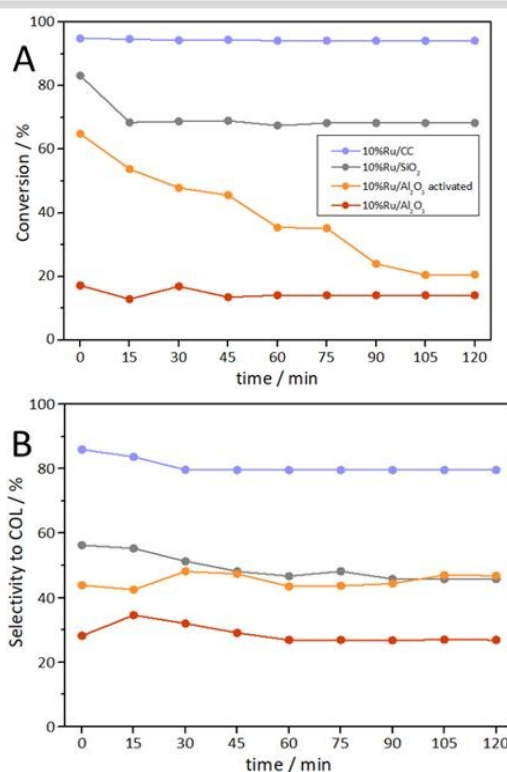
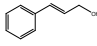
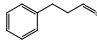


Fig.8 CAL conversion (A) and COL selectivity (B) using different catalysts. Reaction conditions: p = 30 bar H₂; T = 90 °C; flow rate = 0.1 mL min⁻¹

Table 5 CAL conversion and COL selectivity average at stationary state (TOS=120 min) for different supporting materials

Catalyst	Conversion / %	Selectivity / %			Yield to COL / %
				Others	
10%Ru/CC	94	78	22	0	75
5%Ru/CC	64	87	13	0	54
2.5%Ru/CC	28	83	17	0	23
1%Ru/CC	15	62	38	0	10
0%Ru/CC	5	54	46	0	0
10%Ru/SiO ₂	68	32	68	0	22
10%Ru/Al ₂ O ₃ activated	45	45	55	0	25
10%Ru/Al ₂ O ₃	15	28	72	0	10

		COL	HCAL	HCOL		
Blank	<5	-	-	-	-	-
10%Ru/CC	94.4	79.7	-	9.2	11.1	75.2
10%Ru/SiO ₂	68.4	47.4	1.4	2.4	47.8	32.4
10%Ru/Al ₂ O ₃ activated*	20.5	45.3	17.1	3.4	34.2	9.3
10%Ru/Al ₂ O ₃	14.2	28.7	34.3	0	37.0	4.1

*stationary state reached after 105 min

View Article Online
DOI: 10.1039/C9GC01596E

On the other hand, the acidic properties of activated Al₂O₃ enhanced the hydrogenation reaction of CAL, but with low selectivity to COL. Furthermore, such acidity was slowly deactivated in time, reducing the catalytic activity of the catalysts to the same of standard Al₂O₃. This comparison also demonstrated that Ru/CC catalysts could hydrogenate the aldehyde of the α,β -unsaturated aldehyde, while the olefinic bond was hydrogenated only when the compound was in the form of the α,β -unsaturated alcohol. As a consequence, the high activity and selectivity of 10%Ru/CC could be explained in terms of enhanced charge transfer between the metal and the support material (as also indicated and found by XPS analysis) and by the presence of traces of metallic promoters present in the scrap waste CC (mainly Fe, Ce, Zr, Ti, Zn, Pt, Mg and Pd).

Comparison with commercially available hydrogenation catalysts

The catalytic activity of the synthesized scrap-based catalysts was eventually compared with commercially available 5%Pd/C and 5%Ru/C systems, as shown in Fig.9.

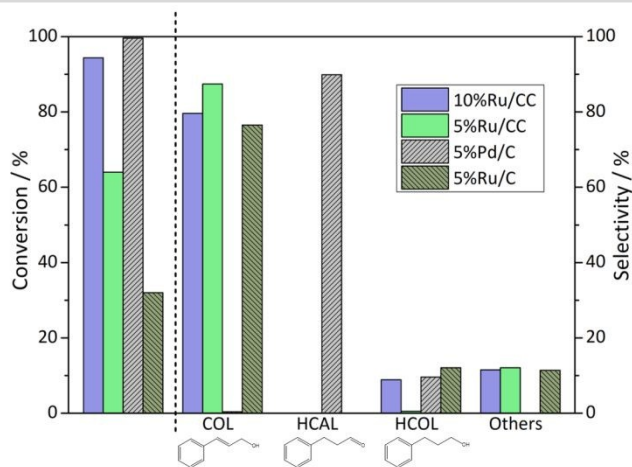


Fig.9 CAL conversion and COL, HCAL, HCOL selectivity average in stationary state (TOS = 120 min) comparing 10%Ru/CC and 5%Ru/CC with commercially available 5%Pd/C and 5%Ru/C. Reaction conditions: p = 30 bar H₂; T = 90°C; flow rate = 0.1 mL min⁻¹

For a complete comparison, also sample 5%Ru/CC was considered, in order to relate the same weight amount of metal loaded. As illustrated in Fig.9, 5%Pd/C was highly active for the hydrogenation, exhibiting an almost complete conversion of CAL under the investigated reaction conditions. Comparably, 5%Ru/CC and 10%Ru/CC were significantly less active. However, Pd was found to be selective to the reduction of the double bond of the α,β -unsaturated aldehyde, favouring

the production of HCAL, which was sequentially hydrogenated to HCOL. On the other hand, Ru/CC catalysts were highly selective to the carbonyl group of CAL. The conversion obtained with 5%Ru/CC was remarkably superior that of 5%Ru/C commercial catalyst (Fig. 9), demonstrating again the positive influence of the catalytic converter supporting material on the catalytic activity.

Stability of the catalyst

The long term stability of 10%Ru/CC was investigated under optimum continuous flow conditions. The reaction was performed for a 10 hours TOS. No relevant changes in conversion of CAL and selectivity to COL demonstrated a good stability of the catalyst under the investigated conditions, as shown in Fig.10, further supported by almost negligible Ru leaching (<10 ppm in the filtrate after 10 h reaction) as determined by ICP-MS.

E-factor

In order to validate the green credentials of the proposed methodology, the E-factor of 10%Ru/CC was calculated and compared to catalysts previously described for the same application.⁵⁸⁻⁶⁰ E-factor was calculated as reported by R. Sheldon:⁶¹

$$E - factor = (total\ waste / kg) / (product / kg)$$

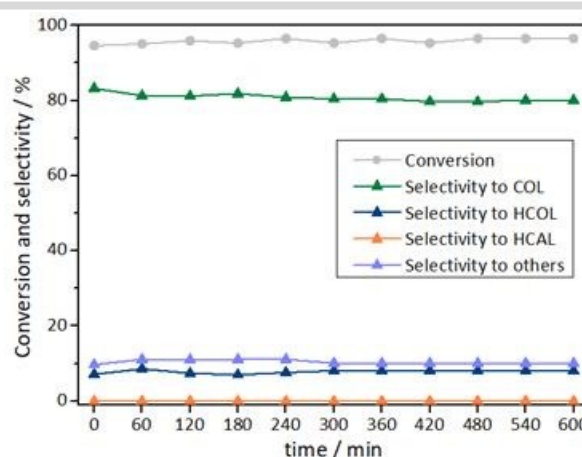


Fig.10 Stability test of sample 10%Ru/CC. Reaction conditions: p = 30 bar H₂; T = 90°C; flow rate = 0.1 mL min⁻¹

While 10%Ru/CC had an E-factor of 24 (which correspond to the industrial segment of fine chemicals), our previously

reported Pd system had an E-factor of 140 (mostly due to the synthesis of the supporting material SBA-15).⁵⁸ Other catalysts, such as Cu–Ni–AAPTMS@GO and CeO₂–ZrO₂ composites supported Pt nanoparticles, have E-factors of <350 and <250, respectively.^{59–60}

4. Conclusions

Ruthenium-based catalysts supported on ceramic-cores of scrap automotive catalytic converters were efficiently synthesized by a mechanochemical approach followed by a chemical reduction. The interaction between Ru and the recycled catalytic converter strongly influenced the catalytic performances of ruthenium. Such catalytic response could be associated with an enhancement of charge transfer and the presence of noble metal particles. Synthesized catalysts were tested in the selective conversion of CAL to COL in continuous flow conditions. A complete analysis of the reaction was performed changing the flow rate and metal loading catalysts. In order to prove the effective influence of the catalytic converter support on the conversion of CAL, different catalysts were prepared using same Ru-loading on standard supporting materials.

In conclusion, a Ru loading of 10%wt allowed the best catalytic performance, including the conversion of CAL up to 95%, with selectivity to COL up to 80%.

This work opens to the possibility of reuse scrap automotive catalytic converters as efficient support materials (for catalyst design) and even as catalysts, to be reported in due course.

Conflicts of interest

The authors declare no conflicts of interest.

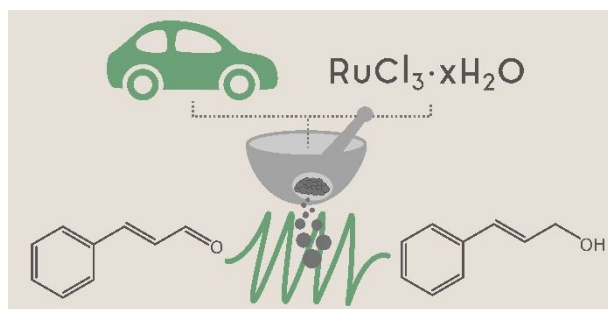
Acknowledgements

The authors thank Mr. Rafael Ángel Gómez Haro and *Provaluta España Reciclaje de Metales, S.L.*, Córdoba (ES), for the supply of scrap automotive catalytic converters. The authors thank Prof. Victor Sebastian, from University of Zaragoza, for HRTEM studies conducted at the Laboratorio de Microscopias Avanzadas, Instituto de Nanociencia de Aragon, Universidad de Zaragoza, Spain. This project has received funding from the European Union's Horizon 2020 research and innovation programme under the Marie Skłodowska-Curie grant agreement No 721290. This publication reflects only the author's view, exempting the Community from any liability. Project website: <http://cosmic-etn.eu/>. The publication has been prepared with support from RUDN University program 5-100.

References

- N. M. Bertero, A. F. Trasarti, B. Moraweck, A. Borgna and A. J. Marchi, *Appl. Catal. A-Gen.* 2009, **358**, 32-41.
- R. Malathi and R. P. Viswanath, *Appl. Catal. A-Gen.* 2001, **208**, 323-327. DOI: 10.1039/C9GC01596E
- C. Milone, M. L. Tropeano, G. Gulino, G. Neri, R. Ingoglia and S. Galvagno, *Chem. Commun.* 2002, 868-869.
- U. K. Singh and M. A. Vannice, *J. Catal.* 2001, **199**, 73-84.
- X. F. Wang, W. M. Hu, B. L. Deng and X. H. Liang, *J. Nanoparticle Res.* 2017, **19**.
- Y. Zhu, H. F. Qian, B. A. Drake and R. C. Jin, *Angew. Chem. Int. Ed.* 2010, **49**, 1295-1298.
- A. B. Merlo, B. F. Machado, V. Vetere, J. L. Faria and M. L. Casella, *Appl. Catal. A-Gen.* 2010, **383**, 43-49.
- L. He, F. J. Yu, X. B. Lou, Y. Cao, H. Y. He and K. N. Fan, *Chem. Commun.* 2010, **46**, 1553-1555.
- P. Gallezot and D. Richard, *Catal. Rev. Sci. Eng.* 1998, **40**, 81-126.
- P. Maki-Arvela, J. Hajek, T. Salmi and D. Y. Murzin, *Appl. Catal. A-Gen.* 2005, **292**, 1-49.
- D. Loffreda, F. Delbecq, F. Vigne and P. Sautet, *J. Am. Chem. Soc.* 2006, **128**, 1316-1323.
- C. J. Kliewer, M. Bieri and G. A. Somorjai, *J. Am. Chem. Soc.* 2009, **131**, 9958-9966.
- W. Koo-amornpattana and J. M. Winterbottom, *Catal. Today*, 2001, **66**, 277-287.
- J. J. Shi, R. F. Nie, P. Chen and Z. Y. Hou, *Catal. Commun.* 2013, **41**, 101-105.
- J. J. Shi, M. Y. Zhang, W. C. Du, W. S. Ning and Z. Y. Hou, *Catal. Sci. Technol.* 2015, **5**, 3108-3112.
- Z. M. Tian, X. Xiang, L. S. Xie and F. Li, *Ind. Eng. Chem. Res.* 2013, **52**, 288-296.
- S. J. Chen, L. Meng, B. X. Chen, W. Y. Chen, X. Z. Duan, X. Huang, B. S. Zhang, H. B. Fu and Y. Wan, *ACS Catal.* 2017, **7**, 2074-2087.
- E. Plessers, D. E. De Vos and M. B. J. Roeffaers, *J. Catal.* 2016, **340**, 136-143.
- A. Y. Hammoudeh, S. M. Sa'ada and S. S. Mahmoud, *Jordan J. Chem.* 2007, **2**, 53-67.
- Y. J. Zhu and F. Zaera, *Catal. Sci. Technol.* 2014, **4**, 3390-3390.
- J. Hajek, N. Kumar, P. Maki-Arvela, T. Salmi, D. Y. Murzin, I. Paseka, T. Heikkila, E. Laine, P. Laukkanen and J. Vayrynen, *Appl. Catal. A-Gen.* 2003, **251**, 385-396.
- J. M. Planeix, N. Coustel, B. Coq, V. Brotons, P. S. Kumbhar, R. Dutartre, P. Geneste, P. Bernier and P. M. Ajayan, *J. Am. Chem. Soc.* 1994, **116**, 7935-7936.
- A. J. Plomp, H. Vuori, A. O. I. Krause, K. P. de Jong and J. H. Bitter, *Appl. Catal. A-Gen.* 2008, **351**, 9-15.
- J. Hajek, J. Warna and D. Y. Murzin, *Ind. Eng. Chem. Res.* 2004, **43**, 2039-2048.
- J. S. Qiu, H. Z. Zhang, X. N. Wang, H. M. Han, C. H. Liang and C. Li, *React. Kinet. Catal. Lett.* 2006, **88**, 269-275.
- G. Neri, L. Bonaccorsi, L. Mercadante and S. Galvagno, *Ind. Eng. Chem. Res.* 1997, **36**, 3554-3562.
- M. Lashdaf, A. O. I. Krause, M. Lindblad, A. Tiitta and T. Venalainen, *Appl. Catal. A-Gen.* 2003, **241**, 65-75.
- Y. Wang, Z. M. Rong and J. P. Qu, *J. Catal.* 2016, **333**, 8-16.
- Y. Wang, Z. M. Rong, P. Zhang and J. P. Qu, *J. Catal.* 2015, **329**, 95-106.
- X. J. Ni, B. S. Zhang, C. Li, M. Pang, D. S. Su, C. T. Williams and C. H. Liang, *Catal. Commun.* 2012, **24**, 65-69.
- S. Galvagno, G. Capannelli, G. Neri, A. Donato and R. Pietropaolo, *J. Mol. Catal.* 1991, **64**, 237-246.

32. S. Galvagno, A. Donato, G. Neri, R. Pietropaolo and G. Capannelli, *J. Mol. Catal.* 1993, **78**, 227-236.
33. P. Gao, A. W. Wang, X. D. Wang and T. Zhang, *Catal. Lett.* 2008, **125**, 289-295.
34. F. Q. Leng, L. C. Gerber, M. R. Axet and P. Serp, *Comptes Rendus Chim.* 2018, **21**, 346-353.
35. M. K. Jha, J. C. Lee, M. S. Kim, J. Jeong, B. S. Kim and V. Kumar, *Hydrometallurgy*, 2013, **133**, 23-32.
36. M. A. Barakat and M. H. H. Mahmoud, *Hydrometallurgy*, 2004, **72**, 179-184.
37. M. Baghalha, H. K. Gh and H. R. Mortaheb, *Hydrometallurgy*, 2009, **95**, 247-253.
38. D. J. de Aberasturi, R. Pinedo, I. R. de Larramendi, R. de Larramendi and T. Rojo, *Minerals Eng.* 2011, **24**, 505-513.
39. M. Benson, C. R. Bennett, J. E. Harry, M. K. Patel and M. Cross, *Res. Conserv. Recycling* 2000, **31**, 1-7.
40. C. H. Kim, S. I. Woo and S. H. Jeon, *Ind. Eng. Chem. Res.* 2000, **39**, 1185-1192.
41. N. Hodnik, C. Baldizzone, G. Polymeros, S. Geiger, J. P. Grote, S. Cherevko, A. Mingers, A. Zeradjanin and K. J. J. Mayrhofer, *Nature Commun.* 2016, **7**.
42. F. Gomollón-Bel, *Chem. Int.* 2019, **41**.
43. F. M. Akwi and P. Watts, *Chem. Commun.* 2018, **54**, 13894-13928.
44. L. Vaccaro, D. Lanari, A. Marrocchi and G. Strappaveccia, *Green Chem.* 2014, **16**, 3680-3704.
45. S. L. James, C. J. Adams, C. Bolm, D. Braga, P. Collier, T. Friscic, F. Grepioni, K. D. M. Harris, G. Hyett, W. Jones, A. Krebs, J. Mack, L. Maini, A. G. Orpen, I. P. Parkin, W. C. Shearouse, J. W. Steed and D. C. Waddell, *Chem. Soc. Reviews*, 2012, **41**, 413-447.
46. C. P. Xu, S. De, A. M. Balu, M. Ojeda and R. Luque, *Chem. Commun.* 2015, **51**, 6698-6713.
47. M. J. Munoz-Batista, D. Rodriguez-Padron, A. R. Puente-Santiago and R. Luque, *ACS Sust. Chem. Eng.* 2018, **6**, 9530-9544.
48. J. R. Chelikowsky, N. Troullier, J. L. Martins and H. E. King, *Phys. Rev. B*, 1991, **44**, 489-497.
49. J. Kaspar, P. Fornasiero and N. Hickey, *Catal. Today*, 2003, **77**, 419-449.
50. D. J. Morgan, *Surf. Interf. Anal.* 2015, **47**, 1072-1079.
51. W. Y. Ouyang, M. J. Munoz-Batista, A. Kubacka, R. Luque and M. Fernandez-Garcia, *Appl. Catal. B-Environ.* 2018, **238**, 434-443.
52. C. Bock, C. Paquet, M. Couillard, G. A. Botton and B. R. MacDougall, *J. Am. Chem. Soc.* 2004, **126**, 8028-8037.
53. E. A. Paoli, F. Masini, R. Frydendal, D. Deiana, C. Schlaup, M. Malizia, T. W. Hansen, S. Horch, I. E. L. Stephens and I. Chorkendorff, *Chem. Sci.* 2015, **6**, 190-196.
54. B. Ulgut and S. Suzer, *J. Phys. Chem. B*, 2003, **107**, 2939-2943.
55. M. Todea, E. Vanea, S. Bran, P. Berce and S. Simon, *Appl. Surf. Sci.* 2013, **270**, 777-783.
56. W. Ouyang, A. Yopez, A. A. Romero and R. Luque, *Catal. Today*. 2018, **308**, 32-37.
57. D. Prat, J. Hayler and A. Wells, *Green Chem.* 2014, **16**, 4546-4551.
58. A. Yopez, J. M. Hidalgo, A. Pineda, R. Cerny, P. Jisa, A. Garcia, A. A. Romero and R. Luque, *Green Chem.* 2015, **17**, 565-572.
59. S. Ranaa and S. B. Jonnalagadda, *RSC Adv.* 2017, **7**, 2869-2879.
60. S. Wei, Y. Zhao, G. Fan, L. Yang and F. Li, *Chem. Eng. J.* 2017, **322**, 234-245. DOI: 10.1039/C9CG01596E
61. R. A. Sheldon, *Chem. Ind.* 1992, 903-906.



View Article Online
DOI: 10.1039/C9GC01596E

Mechanochemical preparation of novel catalyst based on Ru-containing scrap catalytic converters for the selective continuous flow hydrogenation of cinnamaldehyde